Oct 17th, 12:00 AM

# Shear Lag Effect on Bolted C-shaped Cold-formed Steel Tension Members

Chi-Ling Pan

Pen-Chun Chiang

Sixteenth International Specialty Conference on Cold-Formed Steel Structures
Orlando, Florida USA, October 17-18, 2002

# Shear Lag Effect on Bolted C-Shaped Cold-Formed Steel Tension Members

Chi-Ling Pan[1] and Pen-Chun Chiang[2]

**Abstract**

This study is concentrated on the investigation of the shear lag effect on cold-formed steel tension members. C-shaped sections with different dimensions tested by using bolted connections were discussed in this study. The comparisons were made between the test results and predictions computed based on several specifications. In order to study the stress distribution at the various locations of the cross section of specimen, the finite-element software ANSYS was also utilized in this research. Based on the experimental results, it was found that the tension strengths of test specimens predicted by the AISC-Code (1999), which takes account of the shear lag effect, provide good agreement with the test values. The predictions according to AISI-Code (1996) and AS/NZS 4600 Code (1996) seem to be overestimated as comparing to the test results. It is also noted that there is quite a discrepancy between the test results and the values predicted by British Standard (1998).

## 1. Introduction

According to the AISC Specification, a tension member can fail by reaching one of two limit states: (1)Excessive Deformation - the load on the member must be small enough that the stress in the cross section is less than the yielding stress of the steel; (2)Fracture – the load on the member must be small enough that the stress in the effective net section is less than the tensile strength of the steel. The main factor considered in the AISC Specification (1999) for computing

[1] Associate Professor, Dept. of Construction Engineering, Chaoyang University of Technology, 168, Gifeng E. Rd., Wufeng, Taichung County, Taiwan, R.O.C.

[2] Research Assistant, Dept. of Construction Engineering, Chaoyang University of Technology, 168, Gifeng E. Rd., Wufeng, Taichung County, Taiwan, R.O.C.

the effective net area is the shear lag effect. Shear lag effect occurs when some elements of the tension member are not connected. This effect reduces the strength of the member because the stresses distributed over the entire section are not uniform (Easterling and Giroux, 1993). The average value of stresses on the net section may thus be less than the tensile strength of the steel. The reduced strength of the member can be expressed as the efficiency of the net section. Research reported by Munse and Chesson (1963) suggests that the shear lag effect can be accounted for by using a reduced net area. Based on this assumption, AISC Specification (1999) states that the effective net area, $A_e$, of such a member is to be determined by multiplying its net area (if bolted or riveted) by a reduction factor U, that is, when the tension load is transmitted only by fasteners:

$$A_e = UA_n \tag{1}$$

where U = reduction factor

$$= 1-\frac{\bar{x}}{L} \le 0.9 \tag{2}$$

$\bar{x}$ = connection eccentricity

L = length of the connection in the direction of loading

Due to the variety of cross sectional shapes for cold-formed steel members, it is not normally possible or convenient to connect each element to the end connection. Currently, the design formulas of the 1996 AISI Specification do not consider the effect of shear lag. So, as described in the AISI Specification, the nominal tensile strength ($T_n$) of axially loaded cold-formed steel tension members is simply determined by the net area of the cross section ($A_n$) and the yield stress of steel ($F_y$):

$$T_n = A_nF_y \tag{3}$$

When a bolted connection is used, the nominal tensile strength is further limited by the capacity specified in Specification Section E3.2 (1996). Based on the research finding by LaBoube and Yu (1995), design equations have been proposed and adopted in AISI Specification Supplement No.1 (1999) to estimate the influence of shear lag. The amended design criteria for the channel and angle sections under axial tension load are listed as follows:

$$P_n = A_eF_u \tag{4}$$

where $F_u$ = tensile strength of the connected part

$A_e$ = $UA_n$, effective net area with U defined as follows:

U = (1) for angle members having two or more bolts in the line of force

$U = 1.0\text{-}1.20\bar{x}/L < 0.9$ but shall not be less than 0.4 (5)

(2) for channel members having two or more bolts in the line of force

$U = 1.0\text{-}0.36\bar{x}/L < 0.9$ but shall not be less than 0.5 (6)

$\bar{x}$ = connection eccentricity (distance from shear plane to centroid of the cross section)

L = length of the connection

In accordance with British Standard: Structural Use of Steelwork in Building – Part 5. Code of Practice for Design of Cold-Formed Sections (1998), the tensile capacity, $P_t$, of a plain channel can be determined from:

$$P_t = A_e p_y \quad (7)$$

where $p_y$ = design strength, should be taken as $Y_s$ (nominal yield strength) but not greater than $0.84U_s$ (nominal ultimate tensile strength)

$A_e$ = effective net area of the net section

$$= \frac{a_1(3a_1 + 4a_2)}{(3a_1 + a_2)} \quad (8)$$

$a_1$ = the net sectional area of the connected leg

$a_2$ = the cross sectional area of the unconnected legs

Equation (7) may only be used when the width to thickness ratios of the unconnected elements are less than 20.

Australian/New Zealand Standard: Cold-Formed Steel Structures (1996) gives formula similar to that in the AISC Specification as shown here as Equation (9). The nominal design tensile strength is determined by the smaller value of Equations 9a and 9b. Instead of using $A_e$, a term of $0.85K_tA_n$ is used in Equation (9b) to express the effective net area.

$$P_t = A_g f_y \quad (9a)$$

$$= 0.85k_tA_nf_u \quad (9b)$$

where $A_g$ = gross area of cross section

$A_n$ = net area of cross section

$f_u$ = tensile strength used in design

$f_y$ = yield stress used in design

$k_t$ = correction factor for distribution of forces

Kulak and Wu (1997) conducted physical tests using single and double angle tension

members to obtain the net sectional strength and thereby examine the shear lag effect. Developing from the tests, the prediction of ultimate load based on the failure mode is proposed by adding the ultimate strength of the critical section of the connected leg and the strength contributed by the critical section of the outstanding leg, resulting in the following formula:

$$P_u = F_u A_{cn} + \beta F_y A_o \tag{10}$$

where $A_o$ = area of the outstanding leg (gross area)

$A_{cn}$ = net area of the connected leg at the critical section

$F_y$ = yield strength of the material

$F_u$ = ultimate tensile strength of the material

$\beta$ = 1.0 for members with four or more fasteners per line in the connection

0.5 for members with three or two fasteners per line in the connection

Holcomb, LaBoube and Yu (1995) studied both angle and channel sections subjected to a tensile load parallel to their longitudinal axis. The primary intent of the test program was to determine the effect of shear lag. It was found that the geometric parameter (t/s') has an influence on the strength of bolted connections of cold-formed steel members. The stress reduction factor is listed as Equation 11.

$$U' = [3.987(t/s') + 0.514][0.5597(\bar{x}/L)^{-0.3008}] \tag{11}$$

where L = connection length

t = thickness of steel sheet

s' = connected width + $\bar{x}$

$\bar{x}$ = distance from the shear plane to the center of gravity of the cross section

## 2. Experimental Study

The test material used in this study is SSC400 sheet steel specified in Chinese National Standard (1994) with a nominal ultimate tensile strength of 41 kgf/mm$^2$ (400 N/mm$^2$) and up. Two different thicknesses, 2.3 mm and 3.2 mm, of sheet steels were used to fabricate the specimens. The material properties of both steels were obtained by tensile coupon tests. The yield stress and tensile strength of the 3.2 mm–thick sheet steel are 306.20 MPa and 431.90 MPa, respectively. And for the 2.3 mm–thick sheet steel, the yield stress and tensile strength are 312.57 MPa and 437.10 MPa, respectively. The fasteners used to connect the C-shaped specimens were ASTM A325T high strength bolts. The nominal diameter (d) of the bolts was 12.7 mm.

**2.1 Specimens**

For the selection of the dimensions of cross sections, the specimens were designed to have a failure type of fracture on the net cross section, so that the shear lag effect can be evaluated. The specimens were also numerically verified to avoid bearing failure of cross section and bearing failure and shear failure of the bolt in accordance with AISI Specification (1996). Four groups of specimens were used to conduct in this study:

Group A: C-shaped section with a nominal overall web width of 100 mm and nominal overall flange width of 50 mm fabricated from 3.2 mm–thick sheet steel (100×50×3.2).

Group B: C-shaped section with a nominal overall web width of 100 mm and nominal overall flange width of 50 mm fabricated from 2.3 mm–thick sheet steel (100×50×2.3).

Group C: C-shaped section with a nominal overall web width of 80 mm and nominal overall flange width of 40 mm fabricated from 3.2 mm–thick sheet steel (80×40×3.2).

Group D: C-shaped section with a nominal overall web width of 80 mm and nominal overall flange width of 40 mm fabricated from 2.3 mm–thick sheet steel (80×40×2.3).

Two C-shaped sections were assembled back to back by using four high-strength bolts. A total of 24 pairs of sections were tested in this study. One half of the specimens (12 pairs of sections) were connected through the webs using two bolts in two lines of force, the other half of the specimens were connected through four bolts in one line in the direction of applying load. The spacing between the centers of bolt holes was chosen to be larger than three times the bolt diameter. The distance from the end of the specimen to the nearest center of bolt holes was designed to be larger than 1.5 times the bolt diameter according to the AISI Specification. All holes were drilled to 14.3 mm in diameter, and were accommodated with 12.7 mm diameter ASTM A325T bolts as a bearing-type connection.

**3.2 Test Setup**

A tensile testing machine with a capacity of 50 tons was used to conduct all the tests. The configuration of test setup is shown in Figure 1. Two C-shaped sections in same group were assembled back to back by using four bolts and were pulled to failure in the opposite direction. The bearing-type connection was adopted in the bolt assembly as specified in Section E3 of the AISI Specification. During the test, two LVDTs (Linear Variable Differential Transformer) were used to measure the axial deformation for each specimen. Strain gages were also attached on the surfaces of specimens to monitor the strain variations through the test. Figures 2 and 3 show the placements of strain gages on the schematic unfolded specimens

connected using two bolts in two lines of force and four bolts in one line of force, respectively. After the test, a statistical analysis was performed to study the difference between the predicted value and the test result for each specimen.

## 4. Evaluation of Experimental Data

Figures 4 and 5 show the stress distributions in the different cross sections under the ultimate loads for the Group B specimens connected using two bolts in two lines of force and four bolts in one line of force, respectively. It can be seen that more shear lag effect can be observed on the specimen connected using two bolts in two lines of force. As expected, the failure mode of net section fracture was observed for the specimens connected using two bolts in two lines of force. A typical failure photo is shown in Figure 6. On the other hand, a combined tearing and bearing failure was found for the specimens connected using four bolts in one line of force.

In this study, the comparisons were only made between the test results and predictions computed based on several specifications for the specimens having net section failure (specimens connected using two bolts in two lines of force) in order to study the shear lag effect. Table 1 summaries the measured dimensions of the cross sections for the specimens having the failure mode of net section fracture.

### 4.1 Comparison with AISI Specification

The predicted values calculated based on the 1996 AISI Code ($P_{n1}$ and $P_{n2}$) and tested values for the specimens are listed in Table 2. The smaller of the computed values ($P_{n1}$) is designated as the design tensile strength as can be seen in column (1) of Table 2. The ratios of tested to computed tensile strengths for each specimen (column (5) of Table 2) are all smaller than unity varying from 0.670 to 0.966. The computed tensile strength, $P_{n1}$, is based on considering the yield stress occurred uniformly in the net section. Due to ignoring connection eccentricity, the predictions of tensile capacity using the 1996 AISI Specification for a member under axial tension seems to be over estimated.

The predicted values calculated according to the AISI Specification Supplement No.1 are listed in column (3) of Table 2. Equation (6) used to compute the predicted values was established mainly based on the consideration of the shear lag effect. It was observed from column (6) of Table 2 that the standard deviation of the tested to computed tensile strengths can be improved, but all values of the tested to computed tensile strength are still smaller than 1.0.

It seems that the amended formula (Equation (6)) also gives an over estimated result for channel members having two or more bolts in the line of force.

### 4.2 Comparison with BS Specification

The comparisons between test values and the computed tensile strength based on the BS Specification are listed in Table 3. The computed tensile strengths listed in Table 3 were calculated according to Equation 7. It can be seen from Table 3 that the mean value of $P_{test}/P_n$ ratios (tested to computed tensile strength ratios) is 1.028 with a standard deviation of 0.185. The scatter between the tested and predicted values of tensile strength is probably due to the lack of consideration of the connection length and type, even though the areas of connected and unconnected elements of the member are considered in the calculation of tensile strength for the BS Specification.

### 4.3 Comparison with AS/NSZ Specification

The predicted tensile strength for each specimen according to the AS/NSZ Specification are listed in column (2) of Table 4. It was observed from Table 4 that the ratios of tested to computed tensile strength for each specimen are between 0.658 and 0.949. The equation (Equation 8) for predicting the tensile strength of a tension member is quite simple and convenient to use. However, failure to consider the connection length may have caused the discrepancies between the tested and computed values of tensile strength.

### 4.4 Comparison with Holcomb Recommendation

The comparisons between the tested and computed tensile strengths based on the Holcomb Recommendation are presented in Table 5. The computed tensile strengths listed in Table 5 were calculated according to Equation 11. The range of values for the ratio of tested to computed values for the specimens with larger width of web is from 0.922 to 1.007. For the specimens with smaller width of web, the ratios varied from 1.116 to 1.265. Thus the tensile strength is under estimated for the specimens with larger width tested in this study.

### 4.5 Comparison with AISC Specification

Table 6 compares tested tensile strengths with values according to the AISC Specification. The predicted tensile strength for each specimen is determined by $P_{n2}$ and listed in column (2) of Table 6. The difference between the computed and tested values is within 10 percent for all specimens as can be seen in column (4) of Table 6. The computed values calculated based on the AISC Specification provide good correlation with the test results. Therefore, the current AISC Specification is a relatively good predictor of the tensile strength for the specimens tested

in this study.

The tensile strength of a C-Shaped section can be evaluated in terms of the ratio of its average stress at ultimate load ($P_{ult}/A_n$) to the ultimate tensile strength ($F_u$) of the material. The ratio is called the net section efficiency, U'. In fact, net section efficiency represents the strength reduction as discussed in Equation 1. Table 7 presents the calculated net section efficiencies (column (1)) and reduction factors computed according to AISC Specification listed in column (2) for the tested specimens. From column (3) of the Table 7, it can be seen that the AISC equation considering the shear lag effect can provide a fair prediction for the specimens tested in this study.

### 4.6 Comparison with Numerical Model

A commercial finite-element analysis software, ANSYS (version of 5.6), was used to evaluate the stress distribution at different cross sections and to compare the structural behavior of the specimen under ultimate load with the test results. Considering the characteristics of nonlinearity, the 3-D 10-Node Isotropic Structural Solid, SOLID 45, was chosen for the element type used to model the specimen. Since the bearing-type bolted connections was adopted in the assembly of specimens, the friction between the connection area of two C-shaped sections was ignored, and it was assumed that the load was transmitted directly to the holes of the specimens by bearing in the bolts. The restraints of the seven bolts that are used to connect the specimen to the support of test frame are assumed to be fixed in three directions (x, y, and z directions) as can be seen in Figure 7. Three loading stages, $0.25A_gF_y$, $0.5A_gF_y$, and $(P_{ult})_{test}$, were used to investigate the stress distribution on the three cross sections shown in Figure 2.

Figure 8 show the comparisons between the computer outputs and test results for the stress distribution of specimen BA-2 under three loading stages. Based on these three figures (Figures, 8a, 8b, and 8c), the following observations are made:

1. Figure 8a shows that the calculated stresses in three sections agree fairly well with the experimental results for the specimen under the load stage of $0.25A_gF_y$.
2. Due to the axial loading, tensile stresses were observed in most segments at three different cross sections. Some segments were affected by the bending stresses because of the eccentricity of connection, in addition, compressive stresses were found in the edge area of flanges (unconnected elements) as can be seen in Figure 8.
3. It was found that the out-of-plane bending behavior affected the stresses in the web area at the end of the specimen as ultimate load was reached. This behavior induced the compressive stresses in the center area of section 3-3 as can be seen in Figures 8b and 8c.

4. It was observed from the tests that the deformation in the flanges is less than that of the web of specimen. On the other hand, the farther the segment from the center line of specimen, the less stress can be obtained. Similar phenomenon can be found in Figure 8. Therefore, an overestimation result can be expected by applying tensile strength, $A_nF_y$, according to 1996 AISI Specification for a member subjected to an eccentric load.

Figure 9 shows the stress distribution of specimen BA-2 under the load stage of $0.25A_gF_y$ from the ANSYS analysis result. As can be expected, the segment having the maximum tensile stress is below the bottom area of the bolt holes. The compressive stresses can be observed in the edge regions of two flanges in Figure 9.

## 5. Conclusions

In order to investigate the effect of shear lag on the C-shaped cold-formed steel sections, four groups of specimens were tested under tension. A total of 24 pairs of sections were tested in this study. Based on the test specimens having the failure mode of net section fracture, the following conclusions can be drawn for the C-shaped cold-formed steel tension members:

1. From observing the strain readings in the test and the simulation results carried out by the ANSYS program, it is apparent that the stress distribution over the entire section of the specimen is not uniform. The stresses in the connected element (web) are larger than the stresses in the unconnected elements (flanges). Thus, the effect of shear lag is demonstrated, and the effect of eccentricity noted
2. It was found that the tensile strengths of test specimens predicted by the AISC Code (1999), which takes into account the shear lag effect, are in the best agreement with the test values. The predictions according to AISI Code (1996), AISI Specification Supplement No.1 (1999), and AS/NZS 4600 Code (1996) seem to be overestimated as compared to the test results. It was also noted that there is quite a discrepancy between the test results and the values predicted by British Standard (1998).
3. For convenience, all members having only two fasteners per line in the direction of stress, the reduction factor U may be taken as 0.75 according to commentary B3 of AISC Specification (1999). However, it was found from observing Table 7 that the values of net section efficiency (U') varied from 0.475 to 0.685 for the tests in this study. Therefore, it is suggested that the reduction factor, U, should only be determined according to AISC Specification (Equation (2)) rather than by the Commentary suggestion in the calculation of tensile strength for C-shaped cold-formed steel sections.

In summary, the tensile strength of a C-shaped cold-formed steel section can be influenced by the shear lag effect. The cross section is termed not fully effective when it is not connected through all elements of the cross section. The tensile strengths of test specimens computed based on the AISC Code (1999) can provide a relatively good prediction. Other shapes like angles need to be investigated to see whether they also meet this finding. The test specimens in this study were fabricated using two C-shaped sections assembled back to back by using four high-strength bolts. If the C-shaped section connects to a gusset plate with much greater thickness, it is believed that the out-of-plane stiffness of the gusset plate enhances the constraints applied to the end of C-shaped section. Future tests can be used to verify this consideration.

## References


1. American Institute of Steel Construction (AISC), "Load and Resistance Factor Design Specification for Structural Steel Buildings," Chicago, Ill., 1999.
2. American Iron and Steel Institute (AISI), "1996 Edition of the Specification for the Design of Cold-Formed Steel Structural Members," Washington, DC, 1996.
3. American Iron and Steel Institute (AISI), "Specification for the Design of Cold-Formed Steel Structural Members with Commentary 1996 Edition Supplement No. 1," Draft Version No. 1, Washington, DC, 1999.
4. British Standard Institute (BSI), "British Standard: Structural Use of Steelwork in Building-Part 5. Code of Practice for Design of Cold-formed Thin Gauge Sections," London, 1998.
5. Chinese National Standard (CNS), "Light Gauge Steels for General Structure," Bureau of Standards, Metrology and Inspection, Ministry of Economic Affairs, CNS 6183, G3122, 1994.
6. Easterling, W. Samuel, and Giroux, Lisa Gonzalez, "Shear Lag Effects in Steel Tension Members," *Engineering Journal*, American Institute of Steel Construction, Inc., Vol. 30, No. 3, pp77-89, 1993.
7. Kulak, G.L. and Wu, E.Y., "Shear Lag in Bolted Angle Tension Members," Journal of Structural Engineering, ASCE, Vol. 123, No. 9, pp1144-1152, 1997.
8. Holcomb, B.D., Yu, W.W., and LaBoube, R.A., "Tensile and Bearing Capacities of Bolted Connections," 2nd Summary Report, Civil Engineering Study 95-1, University of Missouri-Rolla, 1995.
9. LaBoube, R.A. and Yu, W.W., "Tensile and Bearing Capacities of Bolted Connections," Final Summary Report, Civil Engineering Study 95-6, University of Missouri-Rolla, 1995.
10. Munse, W.H., and Chesson, E. Jr., "Riveted and Bolted Joints: Net Section Design," *Journal of the Structure Division*, Proc. ASCE, Vol.89, No. ST 1, pp107-126, 1963.

**Notation**

$A_{cn}$ = net area of the connected leg at the critical section
$A_e$ = effective net area of the net section
$A_g$ = gross area of cross section
$A_n$ = net area of cross section
$A_o$ = area of the outstanding leg (gross area)
$a_1$ = the net sectional area of the connected leg
$a_2$ = the cross sectional area of the unconnected legs
$F_u$ = tensile strength of the connected part
$F_y$ = yield strength of the material
$f_u$ = tensile strength used in design
$f_y$ = yield stress used in design
$k_t$ = correction factor for distribution of forces
L = length of the connection in the direction of loading
$P_n$ = computed tensile strength
$P_t$ = tensile capacity
$P_{ult}$ = tested ultimate strength
$p_y$ = design strength
$T_n$ = nominal tensile strength
t = thickness of steel sheet
U = reduction factor
$Y_s$ = nominal yield strength
s' = connected width + $\overline{x}$
$\overline{x}$ = connection eccentricity

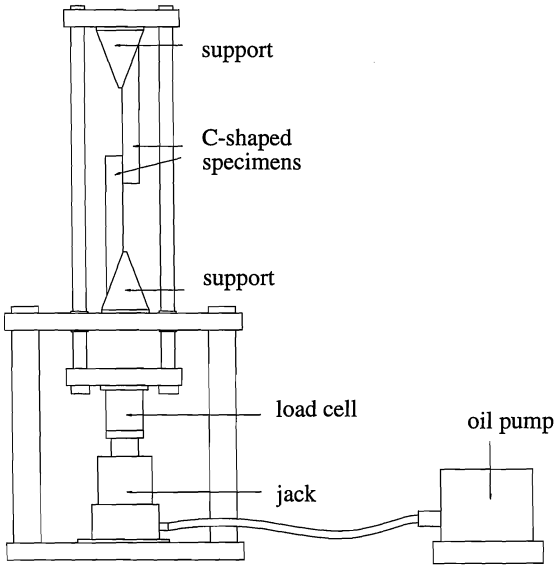


Figure 1 Configuration of Test Setup

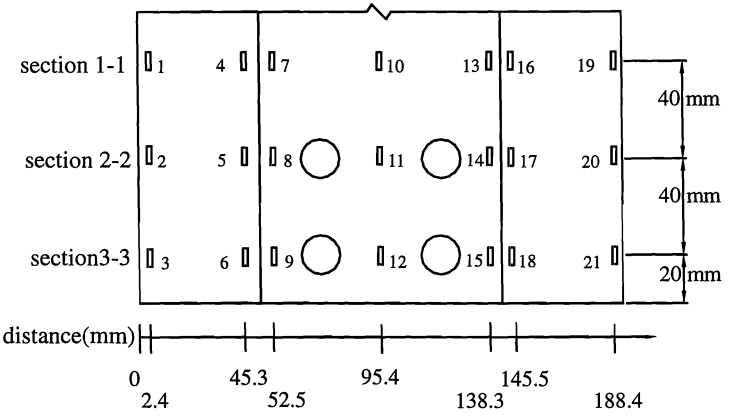


Figure 2 Locations of Strain Gages on the Schematic Unfolded Specimen

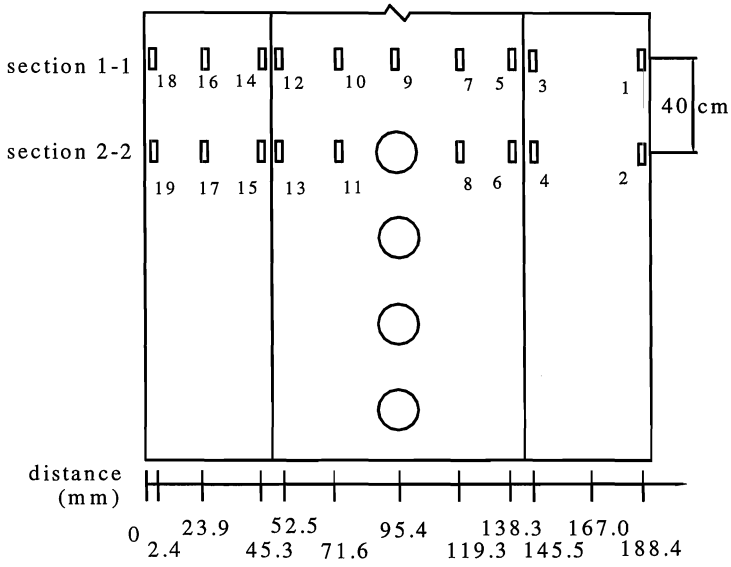


Figure 3 Locations of Strain Gages on the Schematic Unfolded Specimen

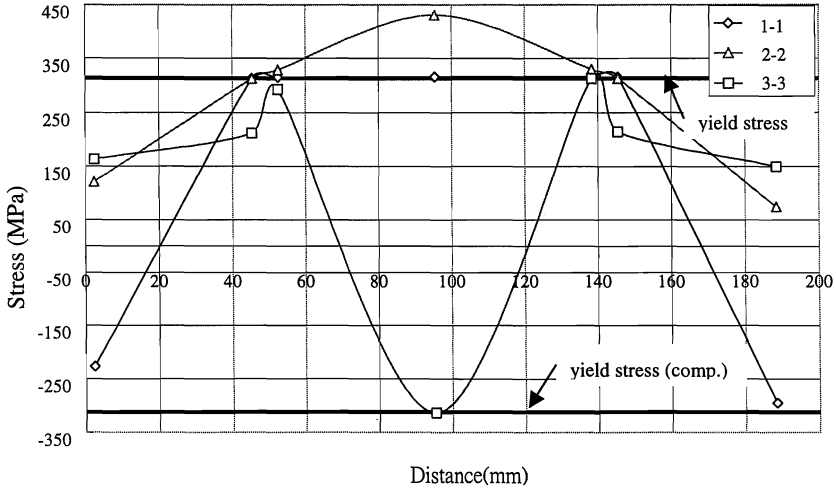


Figure 4 Stress Distributions at Three Cross Sections for Specimen BA-2 under the Load Reaching $(P_u)_{test}$

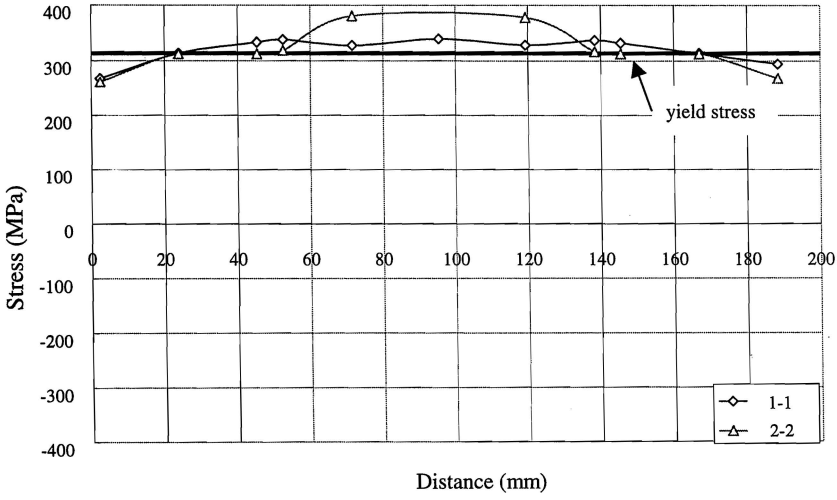


Figure 5 Stress Distributions at Three Cross Sections for Specimen BB-2 under the Load Reaching $(P_u)_{test}$

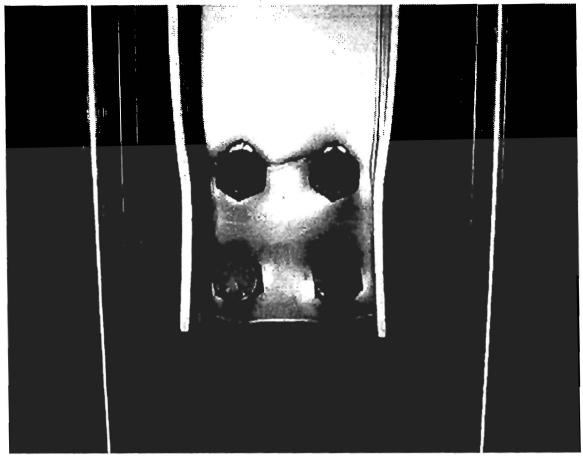

Figure 6 Typical Failure of a Specimen

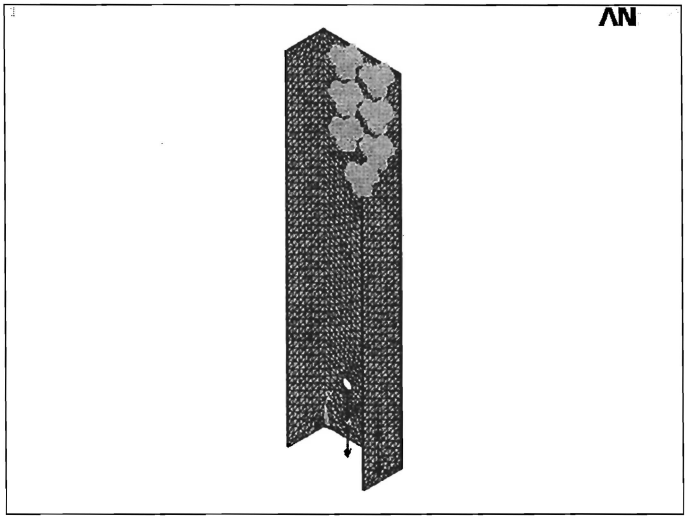

Figure 7 Analysis Model for the Restraint and Loading Settings

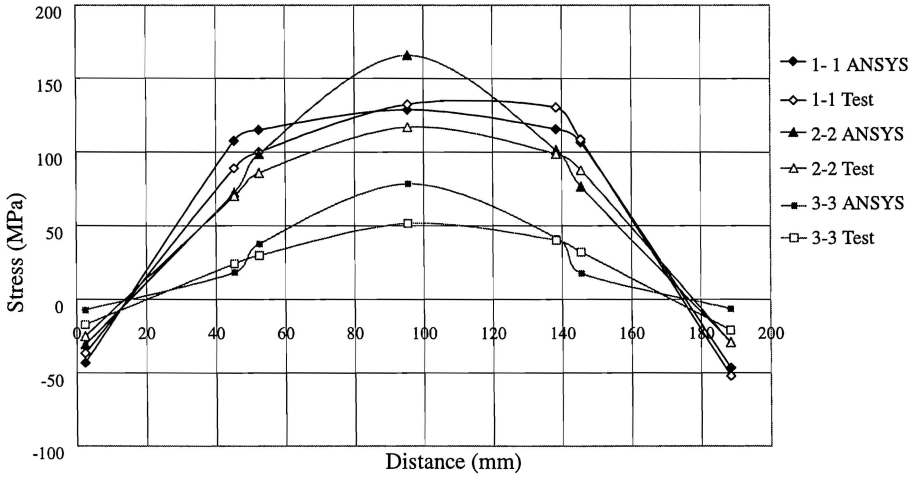


Figure 8a Stress Distributions at Three Cross Sections for Specimen BA-2under a Load Stage of $0.25A_gF_y$

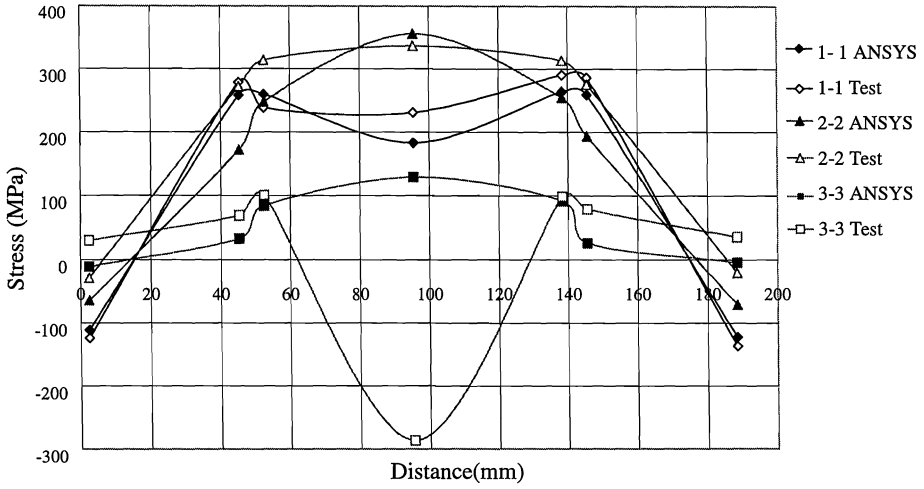


Figure 8b Stress Distributions at Three Cross Sections for Specimen BA-2 under a Load Stage of $0.5A_gF_y$

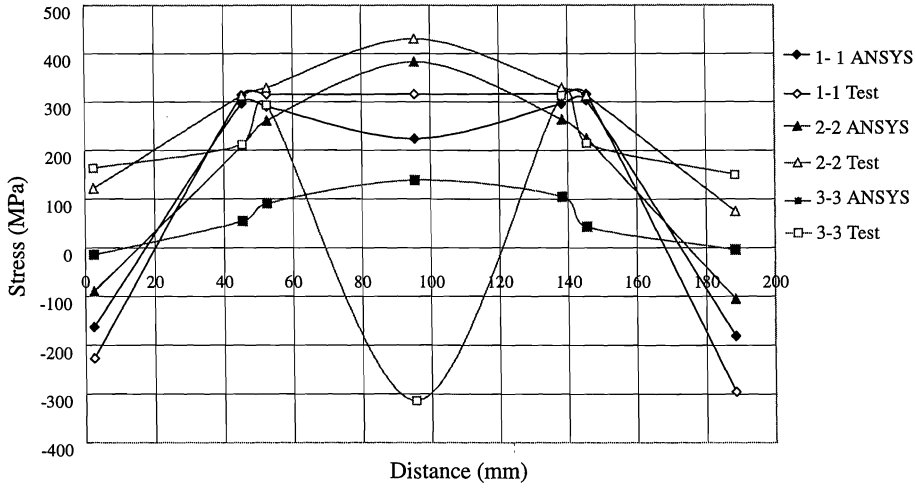


Figure 8c Stress Distributions at Three Cross Sections for Specimen BA-2under the Load Reaching $(P_u)_{test}$

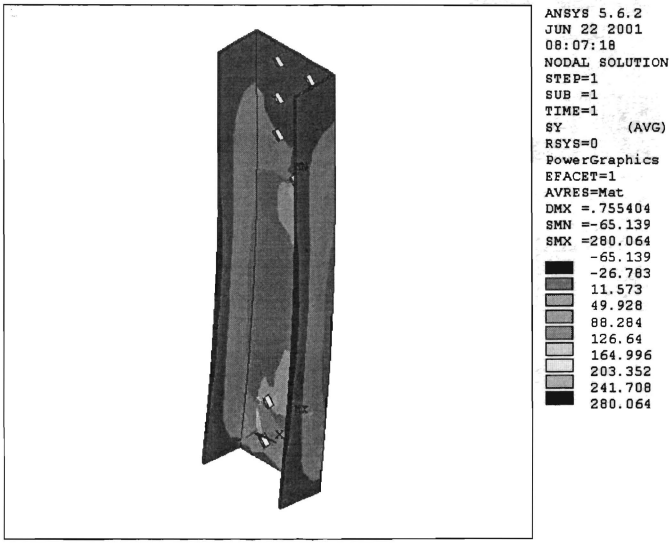


Figure 9 Stress Distribution of the Specimen BA-2 under a load of $0.25A_gF_y$

Table 1 Nominal Dimensions of Cross Sections

| Specimen | H (mm) (1) | W (mm) (2) | t (mm) (3) | R (mm) (4) | $A_g$ ($mm^2$) (5) |
|---|---|---|---|---|---|
| AA-1 | 99.47 | 50.18 | 3.20 | 2.04 | 608.94 |
| AA-2 | 99.60 | 49.98 | 3.20 | 2.04 | 608.08 |
| AA-3 | 99.33 | 50.38 | 3.20 | 2.04 | 609.80 |
| BA-1 | 99.70 | 49.93 | 2.30 | 2.04 | 442.09 |
| BA-2 | 99.93 | 50.08 | 2.30 | 2.04 | 443.35 |
| BA-3 | 100.14 | 49.98 | 2.30 | 2.04 | 443.35 |
| CA-1 | 80.10 | 40.47 | 3.20 | 2.04 | 484.83 |
| CA-2 | 79.82 | 40.43 | 3.20 | 2.04 | 483.65 |
| CA-3 | 80.27 | 40.60 | 3.20 | 2.04 | 486.21 |
| DA-1 | 80.12 | 40.13 | 2.30 | 2.04 | 351.98 |
| DA-2 | 80.12 | 40.13 | 2.30 | 2.04 | 351.98 |
| DA-3 | 79.63 | 40.21 | 2.30 | 2.04 | 351.26 |

Note: H = web overall width, W = flange overall width (average value of two flanges)
t = thickness of steel, R = inside radius of corner, $A_g$ = gross area

Table 2 Comparison of Test Results with AISI Specification

| Specimen | $P_{n1}$ (kN) (1) | $P_{n2}$ (kN) (2) | $P_{n3}$ (kN) (3) | $P_{test}$ (kN) (4) | $P_{test}/P_{n1}$ (5) | $P_{test}/P_{n3}$ (6) |
|---|---|---|---|---|---|---|
| AA-1 | 158.44 | 200.43 | 180.17 | 110.25 | 0.696 | 0.612 |
| AA-2 | 158.17 | 200.10 | 179.87 | 106.08 | 0.671 | 0.590 |
| AA-3 | 158.70 | 200.76 | 180.47 | 110.71 | 0.698 | 0.613 |
| BA-1 | 117.62 | 147.52 | 132.14 | 79.51 | 0.676 | 0.602 |
| BA-2 | 118.02 | 148.02 | 132.58 | 79.05 | 0.670 | 0.596 |
| BA-3 | 118.02 | 148.02 | 132.58 | 81.13 | 0.687 | 0.612 |
| CA-1 | 120.43 | 152.35 | 148.44 | 113.95 | 0.946 | 0.768 |
| CA-2 | 120.07 | 151.90 | 147.99 | 116.03 | 0.966 | 0.784 |
| CA-3 | 120.86 | 152.89 | 148.96 | 115.33 | 0.954 | 0.774 |
| DA-1 | 89.46 | 112.20 | 108.95 | 83.21 | 0.930 | 0.764 |
| DA-2 | 89.46 | 112.20 | 108.95 | 84.59 | 0.946 | 0.776 |
| DA-3 | 89.23 | 111.91 | 108.68 | 85.52 | 0.958 | 0.787 |
| mean | | | | | 0.817 | 0.690 |
| standard deviation | | | | | 0.134 | 0.090 |

Note: $P_{n1} = A_n F_y$, $P_{n2} = (1.0 - r + 2.5\, r\, d / s) F_u A_n$

$P_{n3} = (1.0 - 0.36\, \bar{x}/L) A_n F_u$

Table 3 Comparison of Test Results with BS Specification

| Specimen | $P_n$ (kN) (1) | $P_{test}$ (kN) (2) | $P_{test}/P_n$ (3) |
|---|---|---|---|
| AA-1 | 127.97 | 110.25 | 0.862 |
| AA-2 | 127.96 | 106.08 | 0.829 |
| AA-3 | 127.98 | 110.71 | 0.865 |
| BA-1 | 95.34 | 79.51 | 0.834 |
| BA-2 | 95.66 | 79.05 | 0.826 |
| BA-3 | 95.79 | 81.13 | 0.847 |
| CA-1 | 94.16 | 113.95 | 1.210 |
| CA-2 | 93.74 | 116.03 | 1.238 |
| CA-3 | 94.49 | 115.33 | 1.221 |
| DA-1 | 70.30 | 83.21 | 1.184 |
| DA-2 | 70.30 | 84.59 | 1.203 |
| DA-3 | 69.88 | 85.52 | 1.224 |
| mean | | | 1.028 |
| standard deviation | | | 0.185 |

Note: $P_n = A_e p_y$

Table 4 Comparison of Test Results with AS/NSZ Specification

| Specimen | $P_{n1}$ (kN) (1) | $P_{n2}$ (kN) (2) | $P_{n3}$ (kN) (3) | $P_{test}$ (kN) (4) | $P_{test}/P_{n2}$ (5) |
|---|---|---|---|---|---|
| AA-1 | 186.46 | 161.46 | 200.43 | 110.25 | 0.683 |
| AA-2 | 186.19 | 161.19 | 200.10 | 106.08 | 0.658 |
| AA-3 | 186.72 | 161.73 | 200.76 | 110.71 | 0.685 |
| BA-1 | 138.18 | 118.84 | 147.52 | 79.51 | 0.669 |
| BA-2 | 138.58 | 119.24 | 148.02 | 79.05 | 0.663 |
| BA-3 | 138.58 | 119.24 | 148.02 | 81.13 | 0.680 |
| CA-1 | 148.45 | 122.73 | 152.35 | 113.95 | 0.928 |
| CA-2 | 148.10 | 122.37 | 151.90 | 116.03 | 0.948 |
| CA-3 | 148.88 | 123.16 | 152.89 | 115.33 | 0.936 |
| DA-1 | 110.02 | 90.39 | 112.20 | 83.21 | 0.921 |
| DA-2 | 110.02 | 90.39 | 112.20 | 84.59 | 0.936 |
| DA-3 | 109.79 | 90.16 | 111.91 | 85.52 | 0.949 |
| mean | | | | | 0.805 |
| standard deviation | | | | | 0.132 |

Note: $P_{n1}= A_gF_y$, $P_{n2}= 0.85k_tA_nf_u$, $P_{n3}= (1.0-r_f+2.5r_fd_f/s_f)f_uA_n$

Table 5 Comparison of Test Results with Holcomb Equation

| Specimen | $P_n$ (kN) (1) | $P_{test}$ (kN) (2) | $P_{test}/P_n$ (3) |
|---|---|---|---|
| AA-1 | 115.10 | 110.25 | 0.958 |
| AA-2 | 115.11 | 106.08 | 0.922 |
| AA-3 | 115.09 | 110.71 | 0.962 |
| BA-1 | 80.34 | 79.51 | 0.990 |
| BA-2 | 80.50 | 79.05 | 0.982 |
| BA-3 | 80.58 | 81.13 | 1.007 |
| CA-1 | 97.76 | 113.95 | 1.166 |
| CA-2 | 97.53 | 116.03 | 1.190 |
| CA-3 | 97.96 | 115.33 | 1.177 |
| DA-1 | 67.82 | 83.21 | 1.227 |
| DA-2 | 67.82 | 84.59 | 1.247 |
| DA-3 | 67.58 | 85.52 | 1.265 |
| mean | | | 1.091 |
| standard deviation | | | 0.125 |

Note: $P_n = U'A_nF_u$

Table 6 Comparison of Test Results with AISC Specification

| Specimen | $P_{n1}$ (kN) (1) | $P_{n2}$ (kN) (2) | $P_{test}$ (kN) (3) | $P_{test}/P_{n1}$ (4) |
|---|---|---|---|---|
| AA-1 | 186.46 | 103.16 | 110.25 | 1.069 |
| AA-2 | 186.19 | 102.99 | 106.08 | 1.030 |
| AA-3 | 186.72 | 103.34 | 110.71 | 1.071 |
| BA-1 | 138.18 | 74.65 | 79.51 | 1.065 |
| BA-2 | 138.58 | 74.90 | 79.05 | 1.055 |
| BA-3 | 138.58 | 74.90 | 81.13 | 1.083 |
| CA-1 | 148.45 | 110.32 | 113.95 | 1.033 |
| CA-2 | 148.10 | 109.99 | 116.03 | 1.055 |
| CA-3 | 148.88 | 110.71 | 115.33 | 1.042 |
| DA-1 | 110.02 | 80.26 | 83.21 | 1.037 |
| DA-2 | 110.02 | 80.26 | 84.59 | 1.054 |
| DA-3 | 109.79 | 80.06 | 85.52 | 1.068 |
| mean | | | | 1.055 |
| standard deviation | | | | 0.016 |

Note: $P_{n1} = A_g F_y$, $P_{n2} = A_e F_u$

Table 7 Comparison of Net Section Efficiencies and Reduction Factors

| Specimen | $P_{test}/A_n F_u$ (1) | U (2) | [(1)-(2)]/(2)×100% (3) |
|---|---|---|---|
| AA-1 | 0.493 | 0.462 | -6.29% |
| AA-2 | 0.475 | 0.462 | -2.74% |
| AA-3 | 0.495 | 0.462 | -6.67% |
| BA-1 | 0.483 | 0.454 | -6.00% |
| BA-2 | 0.479 | 0.454 | -5.22% |
| BA-3 | 0.492 | 0.454 | -7.72% |
| CA-1 | 0.671 | 0.649 | -3.28% |
| CA-2 | 0.685 | 0.649 | -5.26% |
| CA-3 | 0.677 | 0.649 | -4.14% |
| DA-1 | 0.665 | 0.642 | -3.46% |
| DA-2 | 0.676 | 0.642 | -5.03% |
| DA-3 | 0.685 | 0.642 | -6.28% |
| average | | | -5.17% |